ELSEVIER

Journal of Chromatography A, 694 (1995) 347–354

JOURNAL OF CHROMATOGRAPHY A

Computational studies on chiral discrimination mechanism of cellulose trisphenylcarbamate

Eiji Yashima, Makiko Yamada, Yuriko Kaida, Yoshio Okamoto*

Department of Applied Chemistry, School of Engineering, Nagoya University, Chikusa-ku, Nagoya 464-01, Japan

First received 19 July 1994; revised manuscript received 17 October 1994; accepted 24 October 1994

Abstract

The calculation of interaction energies between cellulose trisphenylcarbamate (CTPC) and enantiomers of (±)-*trans*-stilbene oxide (**1**) and (±)-*trans*-1,2-diphenylcyclopropane (**2**) was performed using QUANTA/CHARMm and MOLECULAR INTERACTION programs to gain an insight into the chiral recognition mechanism of phenylcarbamate derivatives of cellulose. The structure of CTPC was optimized with the CHARMm force field based on the proposed structure of CTPC by X-ray analysis. In chromatographic enantioseparation on CTPC, **1** was completely resolved ($\alpha = 1.46$) and the (*R*,*R*)-(+)-isomer eluted first followed by the (*S*,*S*)-(−)-isomer, but **2** was not resolved ($\alpha \approx 1$). The results of calculation of interaction energies between CTPC and the enantiomers **1** suggested that the most important adsorbing site of CTPC for **1** may be the NH protons of the carbamate moieties at the 3-position of glucose units, and the (*S*,*S*)-(−)-isomer of **1** may interact more closely than the (*R*,*R*)-(+)-isomer with CTPC. In contrast, there was little difference in the minimum interaction energies between the enantiomers **2**. These calculations agreed with the observed results for the chromatographic resolution on CTPC.

1. Introduction

Understanding chiral recognition at a molecular level is of great interest and importance in many fields of chemistry and biology. Chiral recognition plays an essential role in the field of enantioseparation. Chromatographic enantioseparation has become the most practical way of separating enantiomers, and many chiral stationary phases (CSPs) have been developed [1–4]. Recently, some approaches to the clarification of the chiral recognition mechanism on CSPs for gas and liquid chromatography have been attempted by means of NMR [5–10] and computational methods [8,11–17]. The CSPs that have been most intensively studied in this respect were cyclodextrin-based CSPs [8,9] and Pirkle's type CSPs [11–14]. Based on nuclear Overhauser effect studies, rational models of interactions between the CSPs and enantiomers have been proposed [6,7,10]. The interaction energies between the CSPs and enantiomers were calculated by quantum mechanical calculations [8,11–15,17], and chiral recognition mechanisms have been proposed on the basis of the above calculations and molecular dynamics simulations. Macromolecules such as proteins, polysaccharide derivatives and synthetic chiral polymers have also been used as polymeric CSPs to separate a wide range of racemates and many polymeric

* Corresponding author.

0021-9673/95/$09.50
SSDI 0021-9673(94)01039-0

CSPs are now commercially available [1–4]. However, the chiral recognition mechanism on the polymeric CSPs is still obscure, probably because the polymers usually have a number of different types of chiral binding sites and the determination of their exact structures may be laborious.

Phenylcarbamate derivatives of polysaccharides such as cellulose and amylose appear to be among the most useful polymeric CSPs. They can separate a broad range of enantiomers and give practically useful HPLC columns when they are coated on macroporous silica gel [3]. The chiral recognition mechanism at a molecular level on the polysaccharide-based CSPs is not obvious, although the most important adsorbing site for chiral recognition has been considered to be carbamate residues on the basis of the results of chromatographic enantioseparation. NMR spectroscopy is a useful tool for revealing the chiral recognition at a molecular level, as reported for small-molecule CSPs [5–10], but most of the phenylcarbamate derivatives of polysaccharides with a high chiral resolving power as CSPs are soluble only in polar solvents such as tetrahydrofuran, acetone and pyridine. In such polar solvents, the phenylcarbamate derivatives cannot show high chiral recognition for enantiomers because the solvents must interact strongly with the polar carbamate residues, which are the most important binding site for chiral recognition [18]. Recently, we found that cellulose tris(4-trimethylsilylphenylcarbamate) (CTSP), having a high chiral recognition ability as a CSP for HPLC, is soluble in chloroform, which, for the first time, allowed the chiral recognition mechanism of the phenylcarbamate derivatives to be studied by NMR [19]. In the ^{1}H NMR of (±)-*trans*-stilbene oxide (**1**), methine protons of the oxirane ring were enantiomerically discriminated to show a set of two peaks in the presence of CTSP in $CDCl_3$ [19]. The NMR study of competition experiments with acetone suggests that *trans*-stilbene oxide may be adsorbed on the NH proton of the carbamate residues of CTSP. These NMR studies also indicate that the most important adsorbing sites for effective chiral separation are the carbamate residues, which can interact with enantiomers mainly through hydrogen bonding.

In this paper, we report computational studies on the chiral discrimination mechanism of cellulose trisphenylcarbamate (CTPC). CTPC is the most suitable phenylcarbamate derivatives because its structure has been determined on the basis of X-ray analysis. CTPC shows a high chiral resolving ability as a CSP for HPLC [18]. As a racemate, *trans*-stilbene oxide (**1**) and *trans*-1,2-diphenylcyclopropane (**2**) were selected because **1** has an ether oxygen capable of hydrogen bonding and can be sufficiently separated by HPLC on CTPC, but **2** cannot be resolved on the same column (Fig. 1).

2. Experimental

2.1. Computational methods

Molecular modelling, molecular mechanics (MM) calculations and molecular dynamics (MD) simulations were performed with the

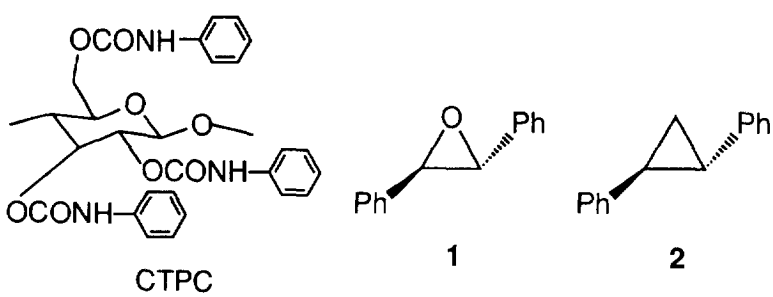

Fig. 1. Structures of CTPC, **1** and **2**.

CHARMm forcefield [20–22] (version 3.2) as implemented in a Polygen's QUANTA/CHARMm program [8,23–28] (Polygen, Waltham, MA, USA) running on a Stellar and a Personal Iris computer (Silicon Graphics). Bond lengths, bond angles, force constants and force field parameters employed in the present calculations were supplied by Polygen. The calculated total energy (E) is expressed in the form

$$E = E_{\text{bond length}} + E_{\text{bond angle}} + E_{\text{dihedral angle}} + E_{\text{improper torsion}} + E_{\text{electrostatic}} + E_{\text{Van der Waals}}$$

The polymer models and the enantiomers **1** and **2** were created by ChemNote in QUANTA. Energy minimizations were performed by steepest descents, followed by conjugate gradient and adopted-basis Newton Raphson minimization. Each step was continued until the value of the "energy value tolerance" became less than 0.001 kcal/mol and all minimizations were carried out using a non-bonded cut-off of 12.0 Å, with a switching window of 7.5–11.5 Å. All energies were given as a root mean square (rms) for a dielectric constant of 1.5. The MD simulation was implemented using Polygen's protocol; heating for 10 ps at 1000 K followed by equilibration for 10 ps with a step size of 0.001 ps.

2.2. Calculation of interaction energy between CTPC and enantiomers

The interaction energies (E') derived from Van der Waals force and electrostatics force between an atom i and an atom j can be calculated with the following equation:

$$E' = E_{\text{electrostatic}} + E_{\text{Van der Waals}}$$

where

$$E_{\text{electrostatic}} = \sum_{i,j>i} (q_i q_j)/(4\pi\varepsilon_0 r_{ij})$$

$$E_{\text{Van der Waals}} = \sum_{i,j>i} (A_{ij}/r_{ij}^{12} - B_{ij}/r_{ij}^{6})$$

q_i and q_j represent electric charge of atoms i and j, respectively, ε_0 is the effective dielectric constant and r_{ij} is the interatomic distance computed from the Cartesian coordinates. The two non-bonded parameters A_{ij} and B_{ij} are derived from the atom polarizabilities and the effective number of outer shell electrons. This calculation is performed for all combinations between the atoms of CTPC and enantiomers.

This energy was obtained by the MOLECULAR INTERACTION program supplied by Polygen. The calculation method using this program is described below. First, a centre of a cubic sampling box is placed on an atom i of CTPC. Here, the size of the cubic sampling box is specified as r. Then, the mesh size is specified as r', and an enantiomer is placed at the grid points and allowed to rotate from 0° to 360° along the x, y and z axes individually at angle (ω_x, ω_y, ω_z) intervals. The interaction energies are calculated for a given set of grid points and (ω_x, ω_y, ω_z).

3. Results and discussion

3.1. Coordinates of racemates and CTPC

The energy minimizations were carried out using the CHARMm force field developed by Brooks et al. [20], which has been widely utilized to construct molecular models of not only biopolymers such as nucleic acids [23,24], polypeptides [25] and synthetic polymers [26], but also small molecules such as cyclodextrin [8] and porphyrin derivatives [28]. The optimized structure of (*S*,*S*)-(−)-*trans*-stilbene oxide [(*S*,*S*)-(−)-**1**] obtained by the MM calculations is shown in Fig. 2. The final energies of both the enantiomers of **1** were 27.54 kcal/mol.

The optimization of CTPC was performed as follows. First, a full energy minimization of one unit of CTPC, containing CH_3O groups at the 1- and 4-positions of a glucose unit, was accomplished in the same way as that for (*S*,*S*)-(−)-**1**. Next, the optimized units were allowed to construct an octamer (8-mer) with a left-handed threefold (3/2) helix according to the structure of CTPC reported by Vogt and Zugenmaier [29] on the basis of X-ray analysis of a CTPC fibre. The dihedral angles defined by H1–C1–O–C4′

Fig. 2. Optimized structure of (*S,S*)-(−)-**1**.

(ϕ) and H4′–C4′–O–C1 (φ) were fixed to be 60° and 0°, respectively, as shown in Fig. 3.

Then, the eight units of CTPC as a starting structure was optimized by the steepest descents method. In the end of the minimization a metastable structure was obtained. The 8-mer has hydrogen bonds between the NH protons of the carbamate moieties at the 6-positions and the carbonyl oxygens at the 2-positions. The distance between the NH proton of the 6-position and the carbonyl oxygen at the 2-position is 2.634 Å. Then the minimization was further performed by using the conjugate gradient followed by the adopted-basis Newton Raphson methods.

The MD simulation was applied to the optimized 8-mer of CTPC. The structures with lower energies were extracted from the trajectory files obtained from the MD simulation and the MM calculations as described above were performed

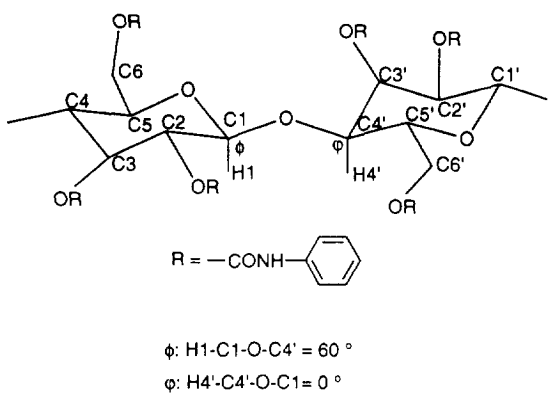

Fig. 3. The linkage of eight units of CTPC.

for these extracted structures again. However, significant changes were not observed before and after MD simulation. The resultant final, most stable, structure is shown in Fig. 4a and b together with the structure of CTPC reported by Vogt and Zugenmaier [29] on the basis of X-ray analysis (Fig. 4c). This structure is more stable than the metastable structure by 1.24 kcal/mol, and the distance between the NH proton and the carbonyl oxygen is 2.724 Å, which is longer than that of the metastable CTPC.

The structure of CTPC in Fig. 4b thus obtained in this study is similar to the structure in Fig. 4c; for example, the side-groups at the 2- and 3-positions and that at the 6-position of the neighbouring glucose unit are close to each other. However, some differences were observed between the calculated and the reported structures. The former is not exactly a 3/2 helix; the rotation angles around at each C1–C4 axis is in the range 110–113° depending on the number of the glucose unit (Table 1), and the conformation between the carbonyl carbon and the ether oxygen of the side-chain at the 2-position is *s-cis*. Further, those at the 3- and 6-positions are *s-trans*, whereas all the conformations of the reported ones are *s-trans*. The conformation of the starting 8-mer before minimization was *s-trans*. Therefore, the conformation at the 2-position was changed to *s-cis* from *s-trans* in the course of the minimization.

3.2. Calculation of interaction energy between CTPC and enantiomers

As mentioned earlier, the most important adsorbing site of CTPC for *trans*-stilbene oxide (**1**) may be the NH protons of the carbamate moieties (Fig. 5).

Therefore, the sampling boxes ($r = 6$, 5, 4 and 3 Å) were placed as centred by the NH proton, then the mesh size (r') was specified as 1 Å, and at each grid point (*R,R*)-(+)-**1** or (*S,S*)-(−)-**1** was rotated at 60° intervals for the x, y and z axes, individually. This means that $5^3 \times 6^3$ (= 27 000) times calculations are implemented if $r = 4$ Å. First, the calculations were carried out

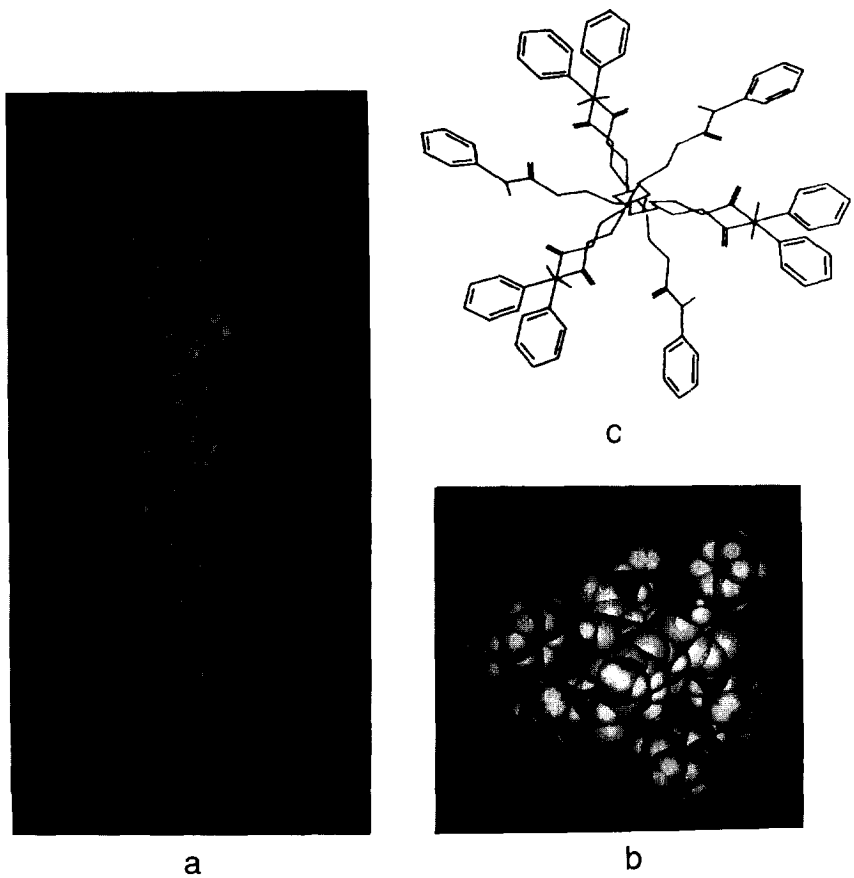

Fig. 4. (a and b) Optimized and (c) reported structures of CTPC. (a) Perpendicular to the chain axis; (b) and (c) along to the chain axis.

at $r = 3$–6 Å and $r' = 1$ Å, and it became clear that when r was 3 Å, the lowest interaction energy was over 100 kcal/mol. When r was 5 or 6 Å, the sampling boxes seemed large enough, and $r = 4$ Å was found to be suitable for the calculation of the interaction energies between CTPC and (±)-**1**. Such a box ($r = 4$ Å) centred by the NH proton covers the area as shown in Fig. 5.

Table 1
Dihedral angles of O–Cl–Cl′–O

Glucose No.	Dihedral angle (°)
1–2	112
2–3	110
3–4	112
4–5	111
5–6	111
6–7	113
7–8	111

The calculation was carried out at each NH proton at the 2-, 3- and 6-positions of glucose units 3, 4, 5 and 6 (Fig. 6) in order to avoid the influence of the end-groups, since CTPC is a polymer (degree of polymerization ≈ 100).

The results of the calculations are shown in Table 2. The minimum interaction energies were very different depending on the number of the glucose unit and the position of the NH. The interaction energies between CTPC and (*S*,*S*)-(−)-**1** were lower than those between CTPC and (*R*,*R*)-(+)-**1** except on 6–2 (2-position at glucose unit No. 6). This suggests that (*S*,*S*)-(−)-**1** may be more tightly adsorbed than (*R*,*R*)-(+)-**1** on

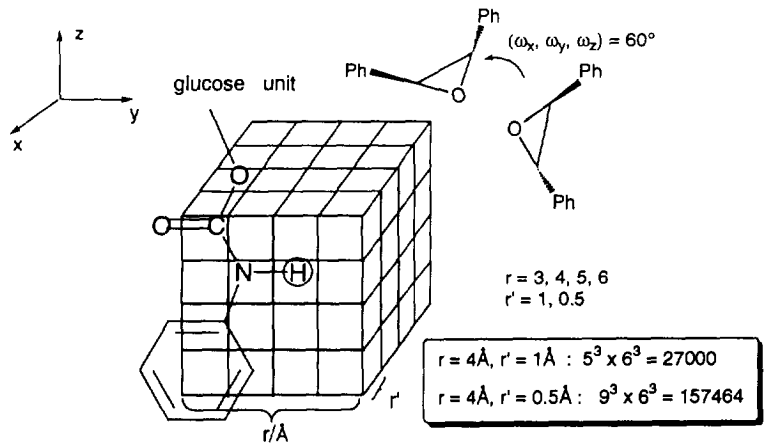

Fig. 5. Method of calculation of interaction energy between CTPC and an enantiomer of **1**.

the CTPC, and that **1** may preferentially interact with the NH protons at the 3-positions of the CTPC because most of interaction energies at the 3-positions were lower than those at the 2- and 6-positions except for glucose unit No. 6. In the chromatographic resolution of (±)-**1** using CTPC as chiral stationary phase, the (*R*,*R*)-isomer elutes first, followed by the (*S*,*S*)-isomer, and the separation factor (α) has been determined to be 1.46 [18]. Therefore, the results obtained by the above calculations are consistent with the results of the chromatographic enantioseparation on CTPC.

Next, a finer sampling box ($r = 4$ Å, $r' = 0.5$ Å) was placed at the NH-proton [4–3 (3-position at glucose unit No. 4)] where the lowest interaction energies appeared for both enantiomers. The results of the distribution of interaction energies are shown in Table 3. The total number of interaction energies under 0 kcal/mol was seven for (*R*,*R*)-(+)-**1** and ten for (*S*,*S*)-(−)-**1**. The lowest interaction energies for (*S*,*S*)-(−)-**1** and (*R*,*R*)-(+)-**1** were −21.42 and −19.10 kcal/mol, respectively. This also indicates that (*S*,*S*)-(−)-**1** may interact more tightly with the CTPC than (*R*,*R*)-(+)-**1**. The calculation described above may still be rough, so to obtain more precise interaction energies at the position 4–3,

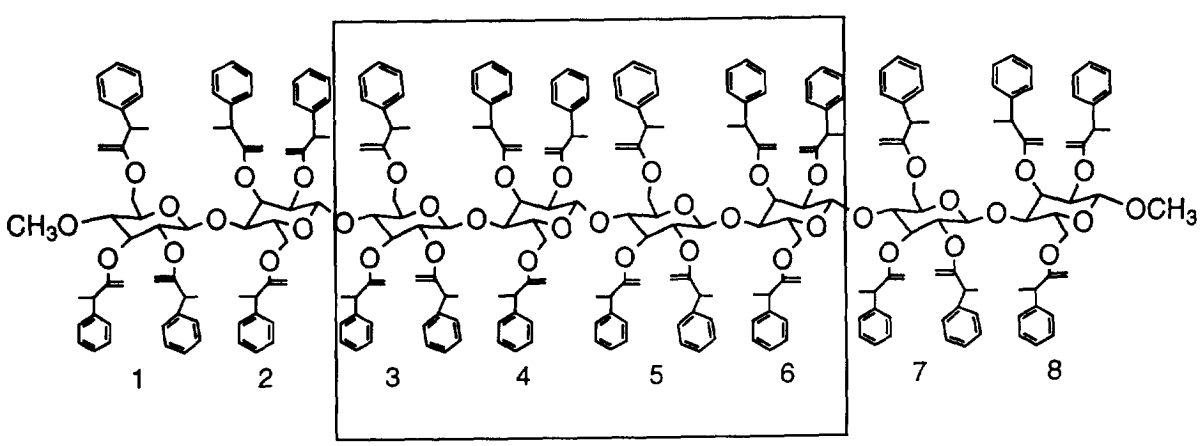

Fig. 6. Octamer of CTPC.

Table 2
Minimum interaction energy between CTPC and **1**

Glucose No. and position	(*R*,*R*)-(+)-**1** (kcal/mol)	(*S*,*S*)-(−)-**1** (kcal/mol)
3–2	–[a]	74.10
3–3	5.62	5.13
3–6	–	–
4–2	32.24	15.53
4–3	17.62	−19.87
4–6	–	–
5–2	23.01	18.14
5–3	−5.87	−7.45
5–6	–	–
6–2	42.72	56.02
6–3	87.42	44.71
6–6	–	46.87

r = 4 Å, r' = 1 Å, 60°; total numbers, 27 000.
[a] Dashes indicate over 100 kcal/mol (1 cal = 4.184 J).

each enantiomer was rotated manually at that point along the x, y and z axes to find the orientations of **1** with lower interaction energies.

The lowest interaction energies between CTPC and (*S*,*S*)-(−)-**1** is −22.16 kcal/mol, whereas that of (*R*,*R*)-(+)-**1** is −19.73 kcal/mol. The decrease in the interaction energies in this operation for (*S*,*S*)-(−)-**1** is 0.74 kcal/mol and that for (*R*,*R*)-(+)-**1** is 0.63 kcal/mol. The difference in the interaction energy between the two enantiomers was 2.4 kcal/mol. This value seems to be large compared with that estimated by the chromatographic separation of (±)-**1** on CTPC. The energy difference ($\Delta\Delta G$) of the interaction between a CSP and a pair of enantiomers is correlated with the α value by $\Delta\Delta G = -RT \ln \alpha$.

Table 3
Distribution of interaction energy between CTPC and (*R*,*R*)- and (*S*,*S*)-**1**

Energy (kcal/mol)	Numbers	
	(*R*,*R*)-(+)-**1**	(*S*,*S*)-(−)-**1**
< −20	0	1
−20 to −10	2	4
−10 to 0	5	5

r = 4 Å, r' = 0.5 Å, 60°; total numbers, 157 464.

Therefore, $\Delta\Delta G$ for α = 1.46 is estimated to be 0.23 kcal/mol. The α value must reflect the sum of the differences in interaction energies between CTPC and a pair of enantiomers. The computer graphics of the interaction between CTPC and (*S*,*S*)-(−)-**1** with the lowest energy is shown in Fig. 7. (*S*,*S*)-(−)-**1** is bound in a chiral groove existing along the main chain of CTPC, and each phenyl group of (*S*,*S*)-(−)-**1** may interact with the phenyl groups of CTPC via π–π interactions and the ether oxygen of the (*S*,*S*)-isomer seems to interact with the NH proton of CTPC via hydrogen bonding. The distance between the ether oxygen of (*S*,*S*)-(−)-**1** and the NH proton of CTPC is 2.502 Å, which is short enough to form hydrogen bonding, while the distance for (*R*,*R*)-(+)-**1** is 3.187 Å. This suggests that (*S*,*S*)-(−)-**1** may interact with the NH proton through the hydrogen bonding, but (*R*,*R*)-(+)-**1** may not interact effectively in such a way.

The same calculation was performed for 1,2-diphenylcyclopropane (**2**). The results of the calculation using the sampling box (r = 4 Å, r' = 1 Å) at glucose units Nos. 4 and 5 suggest that there was little difference in the minimum interaction energies between the enantiomers. The lowest interaction energies for (*S*,*S*)-(−)-**2** and (*R*,*R*)-(+)-**2** were −12.68 and −12.22 kcal/mol, respectively, which appeared at the 3-position of glucose unit No. 4. Moreover, the number of the

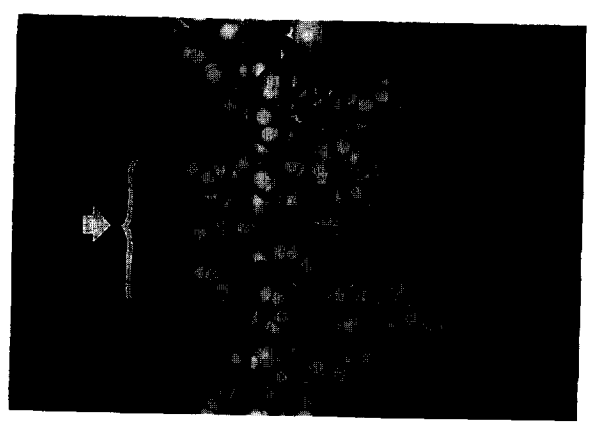

Fig. 7. Computational graphics of the interaction between CTPC and (*S*,*S*)-(−)-**1** (arrowed) exhibiting the lowest energy.

interaction energies under 0 kcal/mol was two for both enantiomers. It is considered that **2** cannot interact with CTPC through hydrogen bonding because of the absence of an ether oxygen as in **1**. The chromatographic resolution of (±)-**2** on CTPC as chiral stationary phase was unsuccessful. This agreed with the results of the chromatographic enantioseparation on CTPC.

4. Conclusions

The interaction energies between CTPC and (*R*,*R*)- and (*S*,*S*)-*trans*-stilbene oxide and between CTPC and (*R*,*R*)- and (*S*,*S*)-1,2-diphenylcyclopropane were calculated by using QUANTA/CHARMm. The results indicate that the most important adsorbing site of CTPC for *trans*-stilbene oxide may be the NH proton at the 3-position and the (*S*,*S*)-isomer may interact more closely with CTPC than the (*R*,*R*)-isomer. The interaction energies between the CTPC and enantiomers of 1,2-diphenylcyclopropane, which has a similar structure to *trans*-stilbene oxide but with no ether oxygen, showed almost no difference.

These calculations agreed with the observed results for the chromatographic resolution on CTPC, although the difference in the calculated interaction energy between the two enantiomers of *trans*-stilbene oxide is large compared with that estimated by the chromatographic enantioseparation. This may be due to the uncertainty in the calculated interaction energy values, which may be dependent on the structure of CTPC. However, we believe that the method reported here may be useful for a qualitative understanding of the chiral recognition mechanism of CTPC. The adaptability of this method to various kinds of enantiomers must be investigated. This approach is not restricted to the study of chiral recognition and should be applicable to a variety of polymer–analyte interactions.

References

[1] S. Ahuja, in S. Ahuja (Editor), *Chiral Separations by Liquid Chromatography* (*ACS Symposium Sereis*, No. 471), American Chemical Society, Washington, DC, 1991, p. 1.
[2] D.R. Taylor and K. Maher, *J. Chromatogr. Sci.*, 30 (1992) 67.
[3] Y. Okamoto and Y. Kaida, *J. Chromatogr. A*, 666 (1994) 403.
[4] W.H. Pirkle and T.C. Pochapsky, *Chem. Rev.*, 89 (1989) 347.
[5] B. Feibush, A. Figueroa, R. Charles, K.D. Onan, P. Feibush and B.L. Karger, *J. Am. Chem. Soc.*, 108 (1986) 3310.
[6] W.H. Pirkle and T.C. Pochapsky, *J. Am. Chem. Soc.*, 109 (1987) 5975.
[7] G.U.-Barretta, C. Rosini, D. Pini and P. Salvadori, *J. Am. Chem. Soc.*, 112 (1990) 2707.
[8] K.B. Lipkowitz, S. Raghothama and J. Yang, *J. Am. Chem. Soc.*, 114 (1992) 1554.
[9] J.E.H. Köhler, M. Hohla, M. Richters and W.A. König, *Angew. Chem., Int. Ed. Engl.*, 31 (1992) 319.
[10] K. Lohmiller, E. Bayer and B. Koppenhoefer, *J. Chromatogr.*, 634 (1993) 65.
[11] K.B. Lipkowitz, D.A. Demeter and C.A. Parish, *Anal. Chem.*, 59 (1987) 1731.
[12] K.B. Lipkowitz, D.A. Demeter, R. Zegarra, R. Larter and T. Darden, *J. Am. Chem. Soc.*, 110 (1988) 3446.
[13] K.B. Lipkowtiz and B. Baker, *Anal. Chem.*, 62 (1990) 770.
[14] S. Topiol, M. Sabio, J. Moroz and W.B. Caldwell, *J. Am. Chem. Soc.*, 110 (1988) 8367.
[15] M.G. Still and L.B. Rogers, *J. Comput. Chem.* 11 (1990) 242.
[16] E. Francotte and R.M. Wolf, *Chirality*, 2 (1991) 43.
[17] T. Hanai, H. Hatano, N. Nimura and T. Kinoshita, *J. Liq. Chromatogr.*, 16 (1993) 801.
[18] Y. Okamoto, M. Kawashima and K. Hatada, *J. Chromatogr.*, 363 (1986) 173.
[19] E. Yashima, M. Yamada and Y. Okamoto, *Chem. Lett.*, 1994, 579.
[20] B.R. Brooks, R.E. Bruccoleri, B.D. Olafson, D.J. States, S. Swaminathan and M. Karplus, *J. Comput. Chem.*, 4 (1983) 187.
[21] F.A. Momany and R. Rone, *J. Comput. Chem.*, 13 (1992) 888.
[22] I.K. Roterman, M.H. Lambert, K.D. Gibson and H.A. Scheraga, *J. Biomol. Struct. Dyn.*, 7 (1989) 421.
[23] D.R. Langley, J. Golik, B. Krishnan, T.W. Doyle and D.L. Beveridge, *J. Am. Chem. Soc.*, 116 (1994) 15.
[24] H.-J. Schneider, T. Blatter, B. Palm, U. Pfingstag, V. Rüdiger and I. Theis, *J. Am. Chem. Soc.*, 114 (1992) 7704.
[25] J.D. Madura, A. Wierzbicki, J.P. Harrington, R.H. Maughon, J.A. Raymond and C.S. Sikes, *J. Am. Chem. Soc.*, 116 (1994) 417.
[26] S.B. Clough, X.-F. Sun, S. Subramanyam, N. Beladakere, A. Blumstein and S.K. Tripathy, *Macromolecules*, 26 (1993) 597.
[27] H.-Y. Zhang, A. Blaskó, J.-Q. Yu and T.C. Bruice, *J. Am. Chem. Soc.*, 114 (1992) 6621.
[28] Ö. Almarsson, A. Sinha, E. Gopinath and T.C. Bruice, *J. Am. Chem. Soc.*, 115 (1993) 7093.
[29] U. Vogt and P. Zugenmaier, *Ber. Bunzenges. Phys. Chem.*, 89 (1985) 1217.